Journal of Energy and Natural Resources
2024, Vol. 13, No. 1, pp. 11-26
https://doi.org/10.11648/j.jenr.20241301.12

Research Article

Reservoir Quality Under the Control of Gravity Flows in the C7 Member of Yanchang Formation in the Jinghe Oilfield, Ordos Basin, China

Yousuf Ah Fudol[1, *], **Hongping Liu**[2]

[1]Graduate School, China University of Geosciences, Wuhan, China

[2]Key Laboratory of Tectonics and Petroleum Resources, Ministry of Education, China University of Geosciences, Wuhan, China

Abstract

The late Triassic sandstone reservoir in the C7 member of the Jinghe oilfield southern Ordos basin is a typical deep-water gravity flow tight oil reservoir. Sedimentary microfacies, physical properties, and petrographic analysis were being examined for quality determination. Pore structure and physical properties data together combined with, thin sections, and scanning electron microscope and core images were used to identify factors controlling reservoir physical properties. The depositional system under debates of different gravity flows including debris flow, seismite slumping, and turbidity flows. Among which sandy debris flow facies shows a better distribution of porosity and permeability followed by seismite-slump, where turbidity facies are the poorest. The petrophysical analysis shows that the study oil interval is a typical tight sandstone reservoir with an average porosity of 9% and permeability average being 0.025mD. The rock classification criteria of the C7 sandstone reveal the sub-categories of lithic feldspar sandstone and feldspar lithic sandstone. Average quartz sandstone contents of 48.25%, average feldspar sandstone content being 25%, and lithic fragments content of 29%. The formation lithology comprises mostly fine-grained sandstone and small pore size, which disclose that the porosity-permeability distribution increases proportional to the average and median pore throat radius, and decreases with average and median pressure. The microfacies distribution shows that the depositional facies controlled physical properties. The sandstone primary pores are affected by the mineral composition of quartz, feldspar, illite, smectite, kaolinite, calcite, and dolomite. Features such as dissolved pores and intergranular pore filling by feldspar, silky-like aggregates of illite-smectite intergranular pore filling and most diagenetic minerals influenced the sandstone pores beside the compaction.

Keywords

Reservoir Quality, Gravity Flows, C7 Member, Yanchang Formation, Jinghe Oilfield

[*]Corresponding author: sudanplus@yahoo.com (Yousuf Ah Fudol)

Received: 7 March 2024; **Accepted:** 26 March 2024; **Published:** 10 May 2024

1. Introduction

Reservoir quality has been broadly studied the past years, in many lacustrine gravity-flow basins [9, 12, 18, 20, 24, 28, 42] recognized that gravity flows reservoirs are effective fields, that receive a great strength of oil reserves [33, 31, 25, 5]. Comparable to conventional reserves, a reservoir under gravity flows presents many challenges in which depositional facies and diagenetic processes control quality [42]. Examining the quality of reservoir rock, it is of attention to consider all the depositional facies, diagenetic change, and mineral cement, that affect on reservoir performance to produce oil successful [31, 35, 42]. Above all, by performing cores, and petrographic study, scholars have studied alterations in reservoir quality of distinctive rock types under different depositional conditions. Hence, variations in reservoir quality have been studied essentially in terms of diagenetic processes, mineral cement, and compaction. Reservoir quality encompasses all the processes that modify in the properties of the sediment from the moment of transport to the deposition ends to the lithification [36, 2]. Importantly, diagenesis and compaction play the vital processes that transform the initial attributes of the clastic rock record [8, 17, 32]. In addition, the mineral assemblage in the clastic rock environment acts with the surrounding circumstances including, climate, burial depth, and adjust the rock properties [2, 11]. Besides the mineral content, the sedimentary environment, rock depositional process and the burial depth, further have a direct impact reservoir pore throat radii [6, 4].

Consequently, with the huge breakthrough in petroleum exploration technologies, it discovered that most of the gravity flow deposits have sequences of the tight reservoirs [43, 38]. In particular, those gravity flow reservoir with fine-grained sediments encountered a mixture of properties that characterized by remarkably low porosity-permeability and oil production [7]. Despite, from for being reservoirs with inadequate physical properties, precisely they have also stacked facies systems and a strong level of diagenetic processes, and mineral cement constitutions that play a considerable impact on reservoir quality [24, 40]. In addition, the gravity flows present high particle combinations, which contributes to support in rock heterogeneities and alter the pore space of reservoir rock [22].

For instance, gravity flow reservoir has far developed in many Chinese marine and none marine petroleum basins e.g., Bohai Basin, and Songliao Basin [19, 39, 21]. It accepted that, reservoirs with a porosity less than 10% and permeability of less than 0.1 mD, considered being a tight reservoir [41, 39, 27]. In the late Triassic of Yanchang Formation of the Ordos Basin, gravity flow reservoirs have explored with low porosity and permeability [30, 44]. The sedimentary sequence of the Yanchang Formation comprises sediment from early to late Triassic which can be subdivided into ten members of C1 to C10, among which the C7 Member is the principal oil-bearing layer in Jinghe Oilfield [23]. It consists lithology of grey to white, fine-grained sandstone, light to grey siltstone and black mudstone and oil shale [16] deposited in a semi-deep water system.

However, the capability to study the quality of the gravity flow reservoir requires quantitative petrophysical and pore structure data interpretation combined with cores. Together, these data define the efficiency of hydrocarbons in a reservoir and specify the capacity of the reservoir. In addition, recognition of depositional facies and property distributions will support in quality decisions for hydrocarbon potential. As a result, limiting the primary control elements of reservoir helps to the rock dynamics that lack to be studied through depositional facies. Despite, the rock porosity and permeability can be influenced by several constitutional factors including diagenesis, depositional environment, mineral cement types and composition [32, 10]. Eventually, many research contributions were taken on reservoir conditions of the C7 Member in the Jinghe oilfield of the Ordos Basin [46, 30]. Considering the earlier researchers, most of the studies were concentrated on sedimentary system descriptions, where fewer studies have been involved to study sandstone quality under gravity flow circumstances. This paper addressed to achieve the quality of the fine-grained sandstone reservoir under the condition of gravity flows in the C7 Member of the Jinghe oilfield. To obtain objectives of the study, adequate cores, thin sections, scanning electron microscope data joint with physical properties and pores structures will build a basic exercise of reservoir quality. Indeed, the study examines the diagenetic evolution and the mineral composition related to the study interval and determine their impact on reservoir quality.

Location and the Geological Settings

The Ordos Basin is the biggest multi-periodic sedimentary basin in the north central of China (Figure 1). The basin surrounded by the eastern to the Jinxi Flexure Zone and the Western thrust belt, where the northern part is next to the Yimeng Uplift, the south to the Weibei Uplift [46, 29, 21], and the central Yishan Slope covers the entire body of the basin. The Ordos is asymmetric-basin trending from north to the south with a gentle dipping slope and a steep dipping west slope [46, 30] with an average of less than 1 ° dip. The Basin experienced extensive tectonic sedimentary evolution from the Paleozoic to the Cenozoic period and a sedimentary sequence during the Early to Middle Triassic Yanchang, in the southern part of the Qinling Belt experienced intracontinental deformation. As a result, the subsidence and deepening of the basin caused a transgression of the lake basin during the Yanchang Late Triassic period. The sediment of this period may be provided from the Yinshan Mountains.

The lake basin development peaked throughout the C7 member period deposition. The amalgamation actions of the fast uplift and steep slopes of the region make favorable con-

ditions for triggering various gravity flows. Despite, the C7 Member now is documented being deposits of the deep-water gravity flows, where seismite-slump sandstones, sandy debris flow sandstones and turbidities current sands can be recognized [30]. Most of all, the Yanchang Formation is the most remarkable oil-production group of the Ordos Basin [34]. It comprises fluvial, deltaic and lacustrine sediments and the sedimentary cycle is divided into five lithologic intervals and ten oil members [23, 15, 45] from C1 Member at the top to the C10 Member at the bottom. After a cycle of the C7 interval, the lake-basin became shallower during the Late Triassic. Lacustrine delta system expanded in the north the central Ordos Basin and produced in the accumulations of fine-grained sandstones and mudstones in the C6 member. The position of the C7 Member of Yanchang late Triassic Formation in the Jinghe Oilfield is in the Binchang region near to the southern Weibei Uplift covers a field over the excess of 3012 km^2.

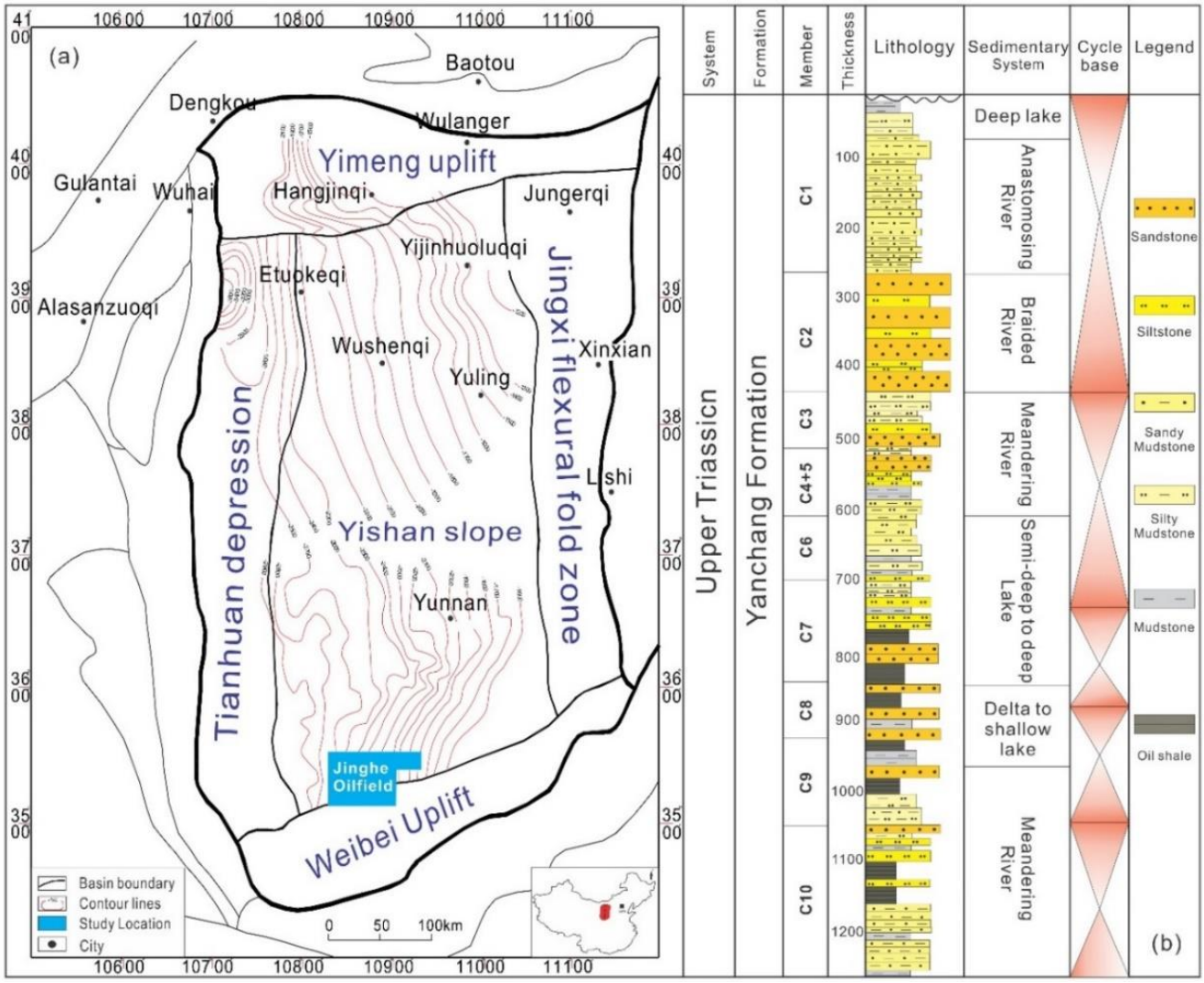

Figure 1. *Location of the Jinghe oilfield and stratigraphic column of the Yanchang Formation in the Ordos Basin.*

2. Reservoir Physical Properties of the C7 Member

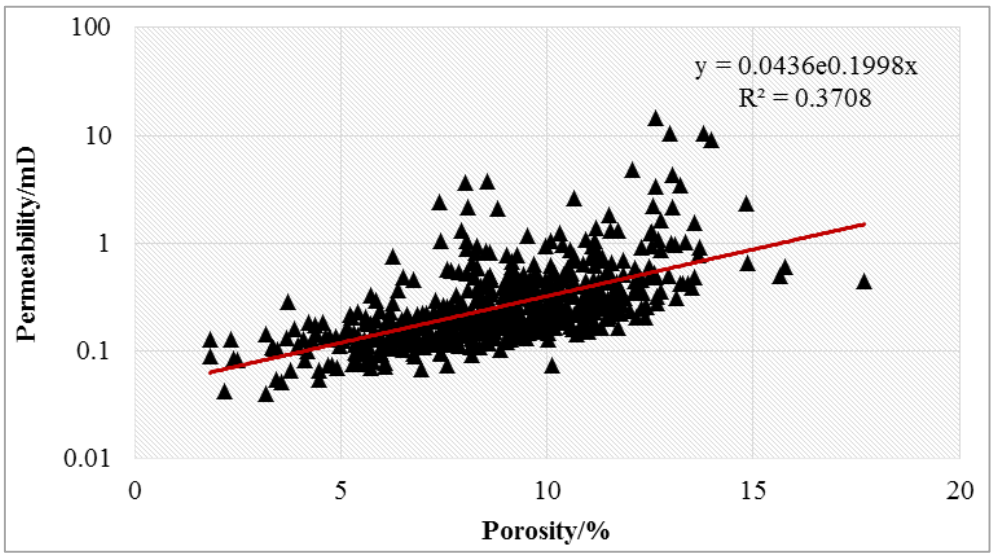

Figure 2. Relationship of porosity and permeability of the C7 member.

Porosity and permeability play two decisive factors that determine reservoir quality. The analysis between porosity and permeability correlations is generally determined by various approaches. The relation between porosity and permeability can be subjective by many factors, such as sediment grain size and the existence of the mineral cement within the reservoir rock. In the present work, the study tested the relationship between porosity and permeability (Figure 2) using the regression cross plot method with a data set of 602 samples. The correlation coefficient of the porosity-permeability was R^2 = 0.3708. This defines that the relation between porosity and permeability is somewhat strong.

Through core description, the C7 Member consists of fine-grained sandstone and siltstone rock deposited in a gravity flow environment. A reservoir with fine-grained sediments under this condition prevailed to diagenetic processes and mineral cement constitutions. These diagenetic processes and mineral composition together with depositional facies may play an important role in sandstone porosity reduction. As explained above, (Figure 3) below displays accumulative distribution of porosity and permeability in the C7 member.

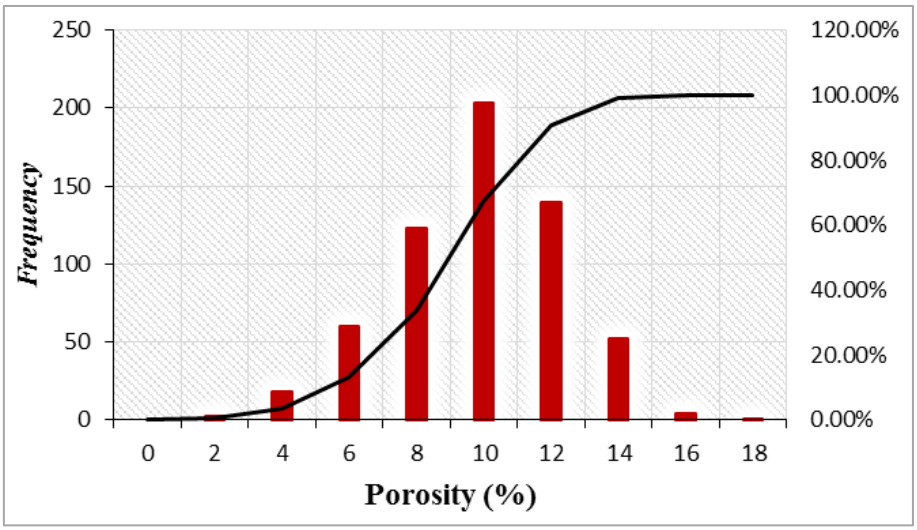

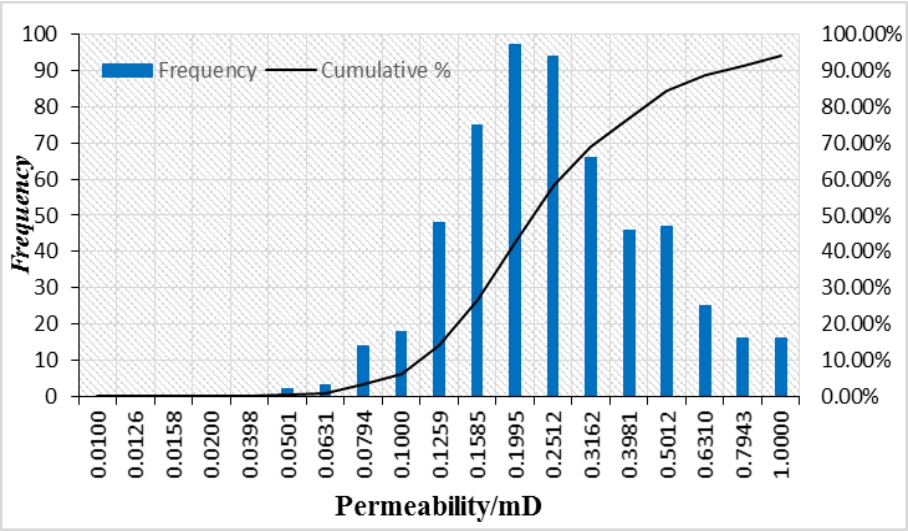

Figure 3. *Porosity and permeability distribution histogram of the C7 Member.*

The C7 Member sandstone has porosity varies from 0 to18%, the average of 9% and permeability varies from 0.01 to 1mD with an average of 0.25mD.

Reservoir Physical Properties Distribution of the C7 Member

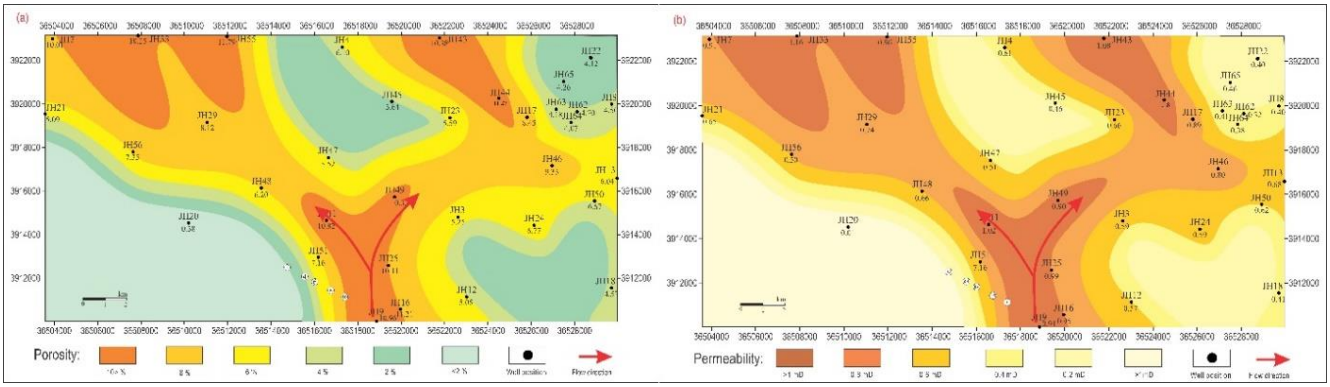

Figure 4. *Physical properties distribution of the C7 member, (a) Porosity and (b) permeability.*

Reservoir physical properties are the most important bounds that require to be considered for sandstone quality assessments. The study linked the porosity and permeability for the C7 member using data gained from porosity-permeability logs (Figure 4). The porosity of the studied member differing from 0.38 to 11.79%, the greater concentration connection noted in the south and the northern areas (Figure 4a). Conversely, the lowest properties connection and distribution indicated in the southeast regions with a porosity of only 0.38%. Undoubtedly, the rock permeability depends upon to the porosity that it involves, the distribution shown in the (Figure 4b). Overall distribution and the tendency demonstrates an analogous distribution to the porosity. It shows permeability values varies from 0.01 to 1.16mD. The further connection and greatest permeability present in the north and the south regions.

The lowest permeability distribution appears in the southwest and the western regions with a permeability of the only 0.01mD. As the permeability is functional to the porosity, and the porosity itself depends on the sedimentary rock category.

The physical properties distribution of the C7 member plays the same tendency of the sedimentary facies distribution; this measures the depositional scheme controls physical properties. The sandy debris flow facies have larger and better distributions of physical properties followed by seismite-slump + turbidite facies. Therefore, the single seismite-slump and turbidity current deposits shows have an inferior connection and poorer physical properties. Besides the depositional facies, the studied oil interval comprises lithology mostly fine-grained sandstone under debate of gravity flows; these fine-grained sediments are categorised by small pore diameter and reasonable physical properties. As a result, sandstones in the deep-water gravity flow system make favoura-

ble conditions in developing mineral cement and diagenetic processes including physical and chemical compaction could change the element of reservoir sandstone.

3. Reservoir Quality of the C7 Member

In order to examine the reservoir capacity; pore structure and porosity-permeability data combined with thin section, scanning electron microscope cores images were utilized to study comprehensively quality of reservoir and figure out the vital control components of the C7 member.

3.1. Sandstone Pore Structure Parameters of the C7 Member

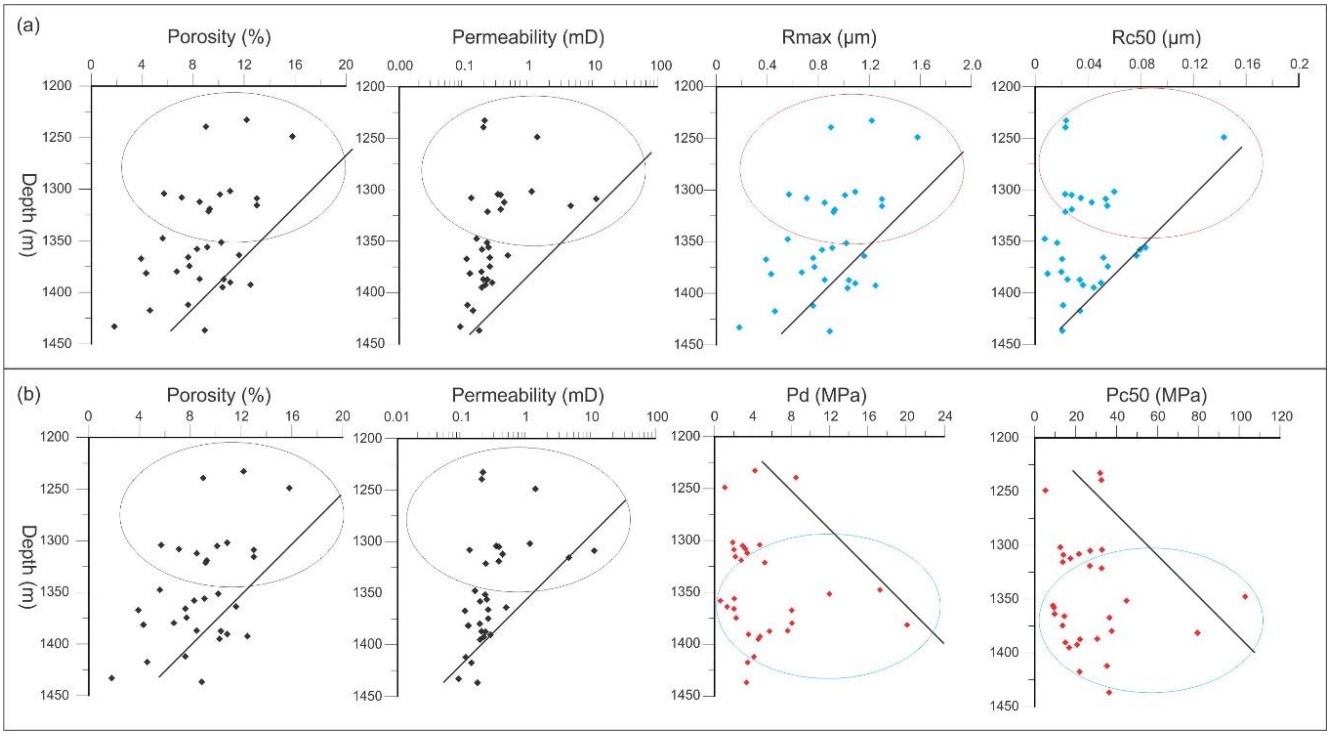

Figure 5. *The relation between pore structure parameter and physical properties with burial depth.*

The most problematic elements that have a considerable affect on reservoir quality by means of physical properties and oil occurrence are rock pores. Certainly, the better pore size depends on the rock grain size, diagenetic evolution and the depositional environment. The C7 Member in the Jinghe oilfield is deposited in a deep-water gravity flow system [13]. Reservoir under these conditions is generally characterised by an extensive variation and complex pore throat. To explain the link between pore throat radii, pore pressure and physical properties, 35 samples comprising the depth of 1450m was used from seven wells study the impact of pore structure on physical properties (Figure 5). These data include; displacement pressure P_d/Mpa, median pressure Pc_{50}/Mpa, average pore throat radius R_{max}/μm, and median pore throat radius Rc_{50}/μm were analysed. The C7 member sandstone marked by small pore volume, average pore throat radius from 0.004 to 0.124μm, and median pore throat radius of 0.007 to 0.143μm. Whereas, the displacement pressure varies from 0.60 to 20.10MPa, and median pressure of 5.23 to 102.97MPa.

As can be seen in the (Figure 5), the statistical test of the C7 member sandstone pore network and physical properties with the burial depth was made. The comprehensive results prove the average pore throat radius and median pore throat radius carries a positive impact on reservoir physical properties. As a result, an increase in the burial depth decreases caused in the reduction porosity-permeability as well as pore throat radii (Figure 5a). Significantly, the relationship of pore pressure shows the negative impact on reservoir porosity and permeability. An increase in burial depth and pore pressure results in a decrease of sandstone porosity and permeability (Figure 5b). In conclusion, the burial depth and pressure gradient have affected the sandstone pores space.

3.2. Lithologic Patterns of the C7 Member

Lithology description is an important duty to reservoir quality identifications; because the rock properties such as

grain size and geometry can affect the physical properties that hold the fluids. Based on core observations, the studied C7 member period composed of three types of lithology (Figure 6), which are fine-grained sandstone, siltstone and argillaceous mudstone and oil shale. The end-member considered as a non-reservoir rock. In relation to the lithology description, cores were described according to their present colour, structures, and bedding features, it believed that the study zone under debates of different gravity flows.

(a) Fine sandstone, massive. Layer C7^{22}, well JH7.

(b) Massive fine sandstone with floating mudstone clasts, layer C7^{22}, well JH7.

(c) Fine sandstone, with slump deformation structure, layer C7^{22}, well JH4.

(d) Fine sandstone with Tron and load structure, layer C7^{21}, well JH4.

(e) Slump deformation fine sandstone, layer C7^{11}, well JH8.

(f) Parallel laminated bedding siltstone. Layer C7^{21}, well JH2.

(g) Liquefied deformation siltstone, layer C7^{12}, well JH2.

Figure 6. *Photographs of some typical gravity flow lithologic patterns in the C7 Member.*

Above all, the depositional condition of the C7 reservoir under debate of gravity flows including; sandy debris flows, slumping flows, and turbidities. Through the core description, fine sandstones identified in the C7 member includes; grey-brown structureless fine-grained sandstone (Figure 6a), a massive fine sandstone with mudstone clasts (Figure 6b) are the major lithological rock type with the other fine-grained sandstone. The lithology and sedimentary structures of these sandstones suggested to the sediments deposited by debris flows.

In addition, grey-to-grey-brown fine-grained sandstone with slump deformation structures also rarely found (Figure 6c). The lithological patterns in these sandstones present a typical feature of sedimentary rock derived by slumping flow. Fine-grained sandstone with random Tron structure and parallel bedding are identified (Figure 6d, and e), these sandstones are mostly white-grey. Therefore, contorted structures and parallel beddings in these sandstones presents evidence

of sediment being transported by turbidity current and traction flows. In the other hand, the siltstone group composed of lithology characterized by light grey to black siltstone with parallel laminations (Figure 6f) and deformation structures (Figure 6g). Sediments with parallel laminae and wavy beddings within the gravity flow deposits presented to the sediment being subjected to mass flow such as slumping and traction flow.

3.3. Sandstone Composition

The sandstone composition analysis in the literature treated in several means [37], but the primary goal is to classify the composition in terms of their belonging to lithologic units. This study analysed the late Triassic C7 Member sandstones following classification criteria of Folk, (1980). However, the samples scattered to illustrate the predominance of litho-clastic rock composition of the reservoir (Figure 7).

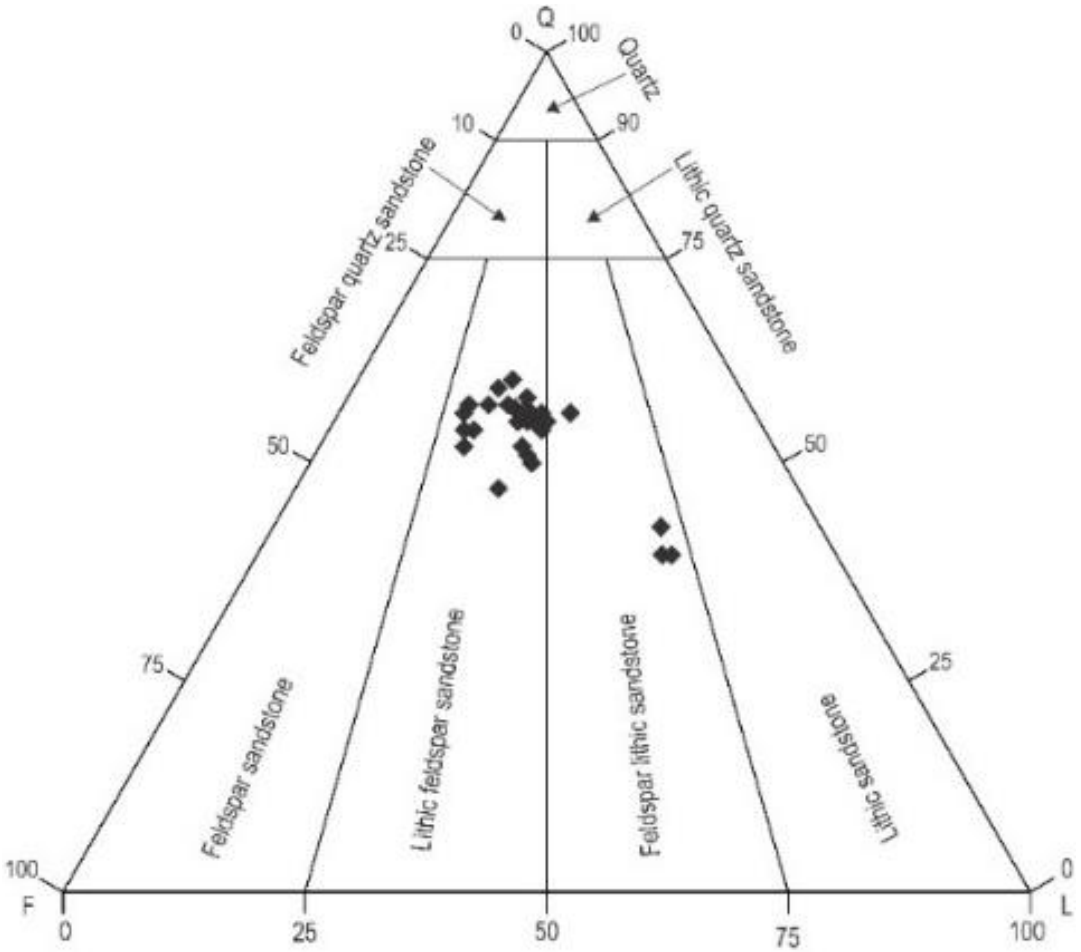

Figure 7. *Sandstone composition and classification diagram of the C7 Member.*

The statistical analysis of core samples from nine wells, the lithic feldspar sandstone, and feldspar lithic sandstone are the principal reservoir rock of the C7 Member. The quartz sandstone contents range from 35.5 to 61%, an average of 48.25%. The feldspar sandstone content ranges from 19 to 31%, an average of 25%. The lithic fragments content of 13 to 45%, an average of 29%.

3.4. Mineral Cement of the C7 Member

In this paper, the study used the petrographic data to reveal the mineral cement associated with the C7 Member and identify how these cement influence on reservoir sandstone quality. Categorising mineral cement within the reservoir sandstone is an important part of reservoir quality evaluation. Because the development of mineral cement could affect the quality of sandstone by introducing substantial fine-grained particle of clays to the pore space [14], which influences primary porosity and permeability of the sandstone rock. Thus, the major authigenic minerals identified from the thin section and electron microscope data includes; quartz, quartz overgrowth, feldspar. Clay cement including; calcite, dolomite, kaolinite, illite, smectite and mixed-layers of illite/smectite cement.

3.4.1. Clay Cement

Clay mineral cement types exhibited in the C7 Member

sandstone are shown in (Figure 8). These cements include; carbonate, kaolinite, illite, smectite, and mixed-layer of illite/smectite. First of all, clay types of cement preserved as external minerals that influence the internal sandstone pores and could reduce the porosity and permeability of the reservoir by filling the intergranular pores. Most of the clay cement identified in the study interval shows aggregates of illite, smectite and kaolinite filling intergranular pores of sandstone.

The clay minerals composition affects the C7 Member sandstone quality in the Jinghe oilfield and creates high complexity and heterogeneity of reservoir sandstone. Minerals cement such as carbonate cement plays the most important diagenetic constituents in a sandstone reservoir quality. In addition, they precipitate within the sandstone rock pores and leads to the pore dissolved pores and compaction. Based on the observation in a scanning electron microscope data, calcite cement was identified with muddy sandstone and stored the clastic rock pores (Figure 8a). It blocks sandstone pores with the face rate of 1-2%. In short, calcite cement caused in the reduction the reservoir sandstone primary pores through compaction.

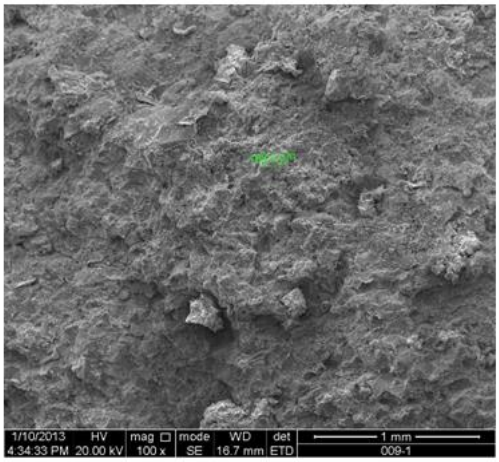

(a) Calcite compactness. Depth; 1356.58, layer $C7^{11}$, Well JH17.

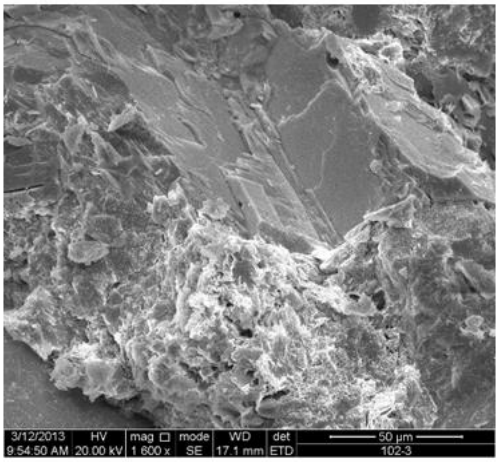

(b) Dolomite and illite cement. Depth; 1339.99, layer $C7^{22}$, Well JH29.

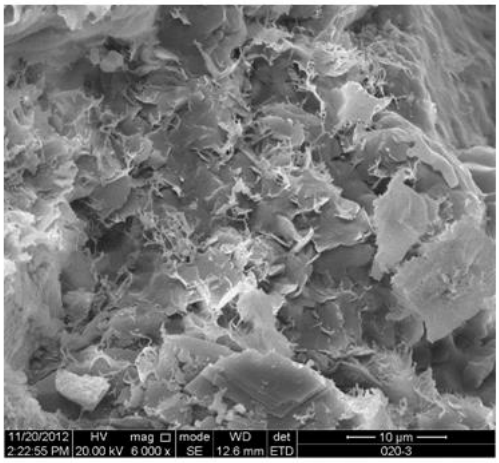

(c) Mixed layers of illite/smectite. Depth; 1392.85. $C7^{11}$ layer, Well JH33.

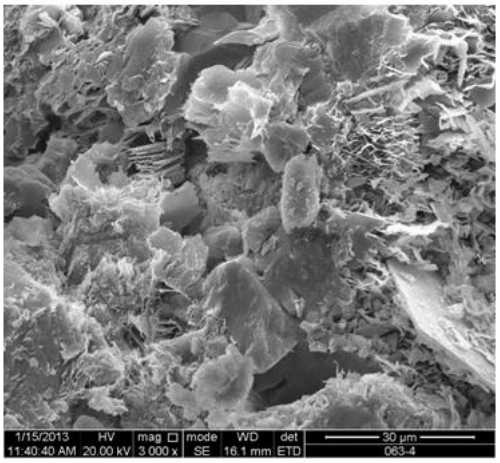

(d) Kaolinite and illite aggregate. Depth; 1010.99, layer $C7^{22}$, Well JH16.

Figure 8. *Photographs of clay cement types in C7 Member of the Jinghe oilfield.*

Smectite and illite types of cement are complex clay minerals in sandstone reservoirs for several reasons. They represent 25% of clay-cemented sandstones [26] that supply material for other diagenetic processes such as mixed-layers of illite/smectite and quartz overgrowth cementation. In addition, they precipitate in sandstone pore network and affect reservoir quality because. Smectite frequently found in fine-grained sediments at low temperatures [1], and illite cement remains accompanying with intensely buried mudstone at high temperatures. Thus, changing in burial depth and the formation temperatures result in a transform of smectite into illite. In a similar way, smectite and illite identified in the C7 Members sandstone show in different forms. They often found mixed-layer of illite and smectite typically shows an irregular shape of a

silk-like structure and filling intergranular pores of sandstone (Figure 8c). Some samples show, mixed-layer of grain filling illite and smectite developed with other clay cements such as calcite (Figure 8d). Kaolinite cement identified with the intense replacement illite and smectite cement. Kaolinite cement precipitation shows in the form of pore filling types associated with illite and smectite cement (Figure 8d).

3.4.2. Authigenic Minerals

Authigenic minerals including quartz overgrowth and feldspar are common in clastic reservoirs to experience diagenesis factors, which influence on reservoir physical properties by the interaction of fluid movements within the clastic rocks (Figure 9). They can also influence the chemical properties of the rock by pore-filling dissolution together with the mechanical compaction and controls on porosity and permeability. Quartz minerals represent 35.5 ~ 61%, of the C7 sandstones. Clearly, two types of quartz minerals observed based on the electron-scanning microscope, which includes detrital quartz, and quartz overgrowth. The detrital quartz minerals shows are flake-like authigenic quartz, filling intergranular pores of sandstone with mixed-layer of illite and smectite (Figure 9a). The quartz overgrowth observed within the reservoir sandstones shows as syntaxial overgrowths with the size of 35.29μm in size (Figure 9b). Obviously, quartz overgrowth faintly filled the intergranular pores of sandstone, associated with mixed-layer of illite and smectite at edges quartz grains.

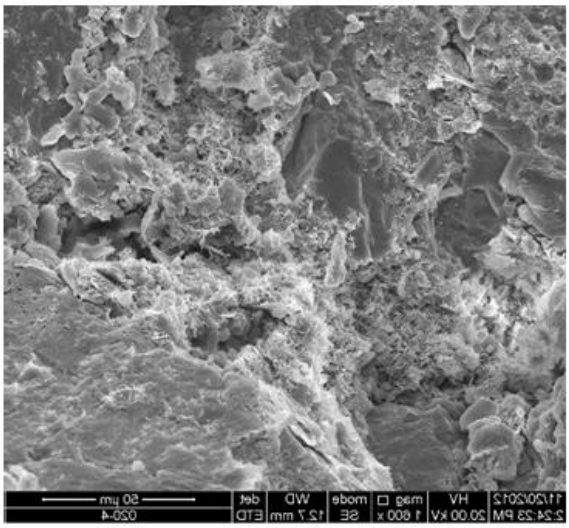

(a) Quartz Intergranular pore filling. Depth; 1392.85, layer $C7^{11}$, Well JH33.

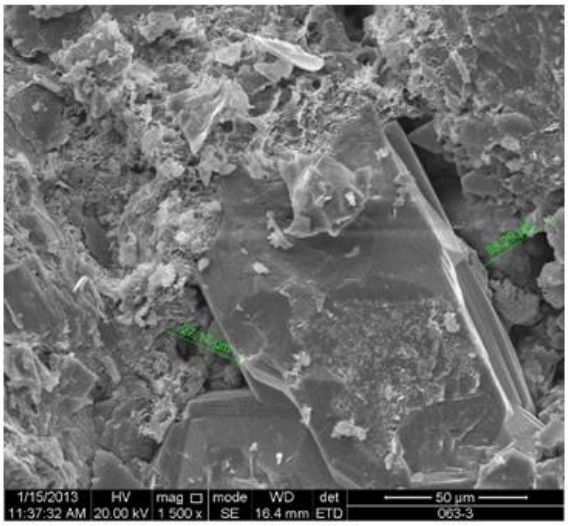

(b) Syntaxial quartz overgrowth. Depth; 1010.99, layer $C7^{22}$, Well JH16.

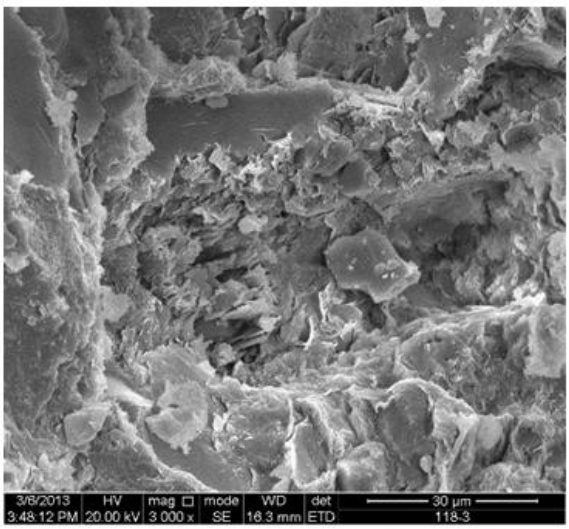

(c) Feldspar and illite pore filling c. Depth; 1435.63, layer $C7^{22}$, Well JH22.

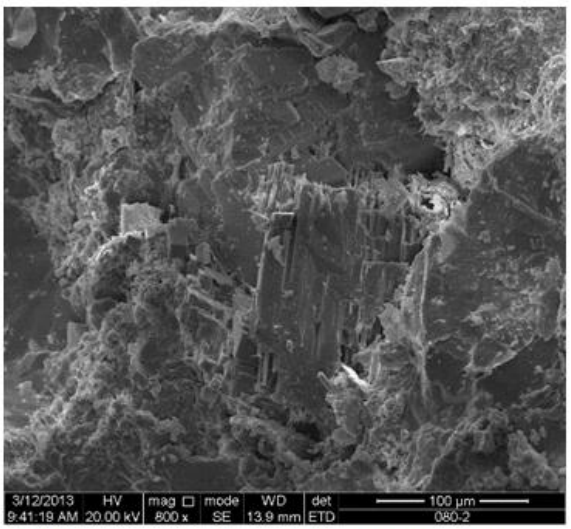

(d) Feldspar dissolved pore. Depth; 1325.91, layer $C7^{11}$, Well JH29.

Figure 9. *Photographs of authigenic mineral cement types in C7 Member of the Jinghe oilfield.*

Feldspar is the most abundant cement in the C7 Member sandstone. Feldspar concentration and existence depends on the burial depth and the surrounding cement types. Based on the sandstone composition analysis, feldspar is 19 to 31% of the rock volume. The aggregate of feldspar also varies with different oil layers and the increasing depth. Most of the feldspars show dissolved pores associated with intergranular pore filling filled (Figure 9c). Whereas, feldspar minerals in some samples, were partially dissolved and filled pores with dolomite (Figure 9d).

3.4.3. Sandstone Diagenesis Features of the C7 Member

Diagenesis comprises processes by which original sedimentary assemblages and interstitial pore waters react with their environment [32]. These processes are active as in terms of temperature and the pressure during the deposition and uplift cycle of the basin history. As illustrations, rock diagenesis encompasses a wide-ranging of post-depositional modifications to sediments, which, includes compaction and lithification of sediments during burial. As explained before, the C7 member is an important oil-bearing unit in the Jinghe oilfield, it forms a part of the Ordos late Triassic Yanchang Formation. Therefore, the depositional period comprises fine-grained sandstones, siltstones and argillaceous mudstone and oil shale dominated by sandy debris flows. Following unconventional petroleum resources theories, a reservoir which has the average porosity being <10%, and permeability average of <1mD is suggested being a tight reservoir (Oluwadebi, Taylor et al. 2018).

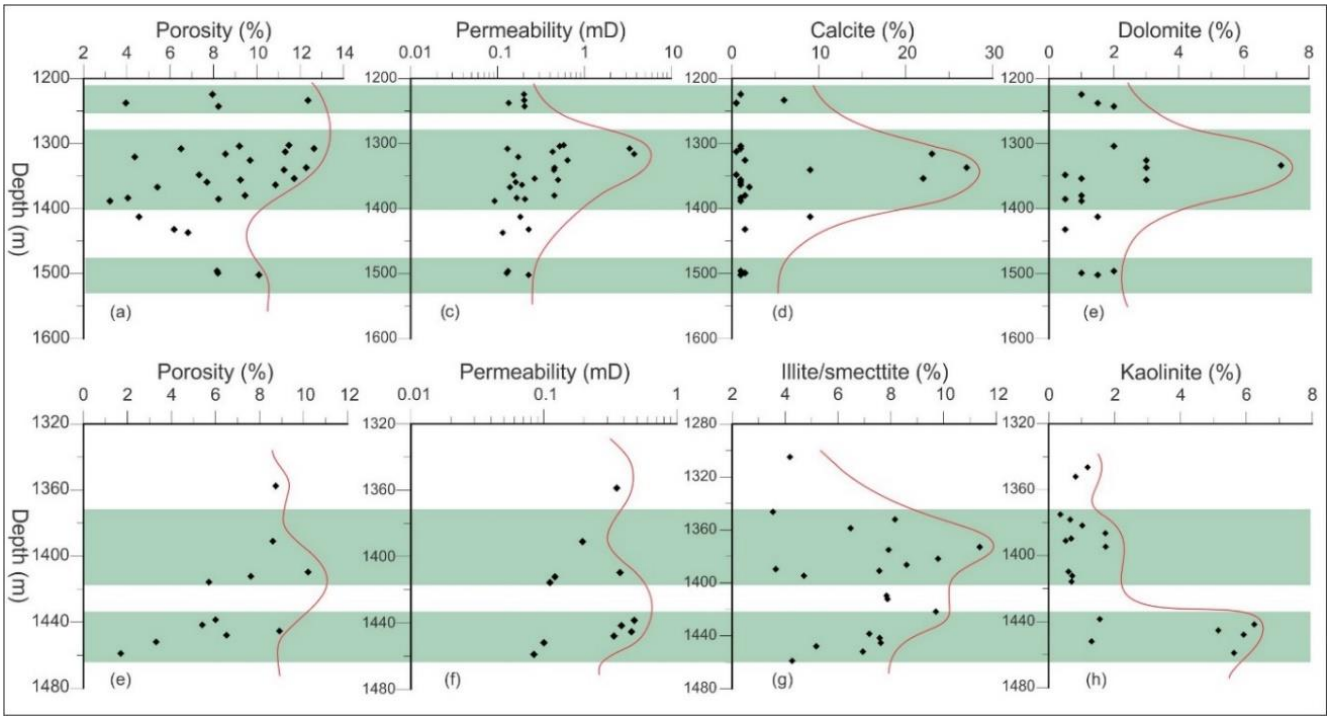

Figure 10. *Effect of clay cement on the porosity and permeability of the C7 member.*

Through the statistical analysis of petrographic data of the C7 Member, sandstone has the average porosity being 9%, and permeability average being 0.25mD. This lower porosity and permeability describes that the study interval is a typical tight sandstone reservoir. Based on the thin section observations, the diagenetic features identified involve compaction and mineral cements including; carbonates (dolomite and calcite), clay minerals (kaolinite, illite and smectite), and authigenic minerals (quartz, and feldspar).

The thin section data observations from six wells, the sandstone quality of the C7 member is under the control of diagenetic and compaction. Three types of diagenetic processes include mineral dissolved pores, compaction and intergranular pore filling cement were identified (Figure 11). Most of the intergranular pore filling minerals dominated by feldspar and dolomite cement. In the (Figure 11a) the intergranular pores of the rock filled by feldspar and dolomite followed by residual intergranular pores with the face rate of about 2-3%. In the (Figure 11b), the filled by feldspar and it dissolved the edge of some particles. In the (Figure 11c), the clastic rock filled with feldspar intergranular pores and mudstone. In the (Figure 11d), shows the mechanical compaction of dolomite and no measurable pores developed in the rock. In the (Figure 11e), feldspar intergranular dissolved pores and debris affected the rock pores where measurable pores in the rock are not developed. In the (Figure 11f) there were no

measurable pores were developed, feldspar and quartz dissolved pore filling.

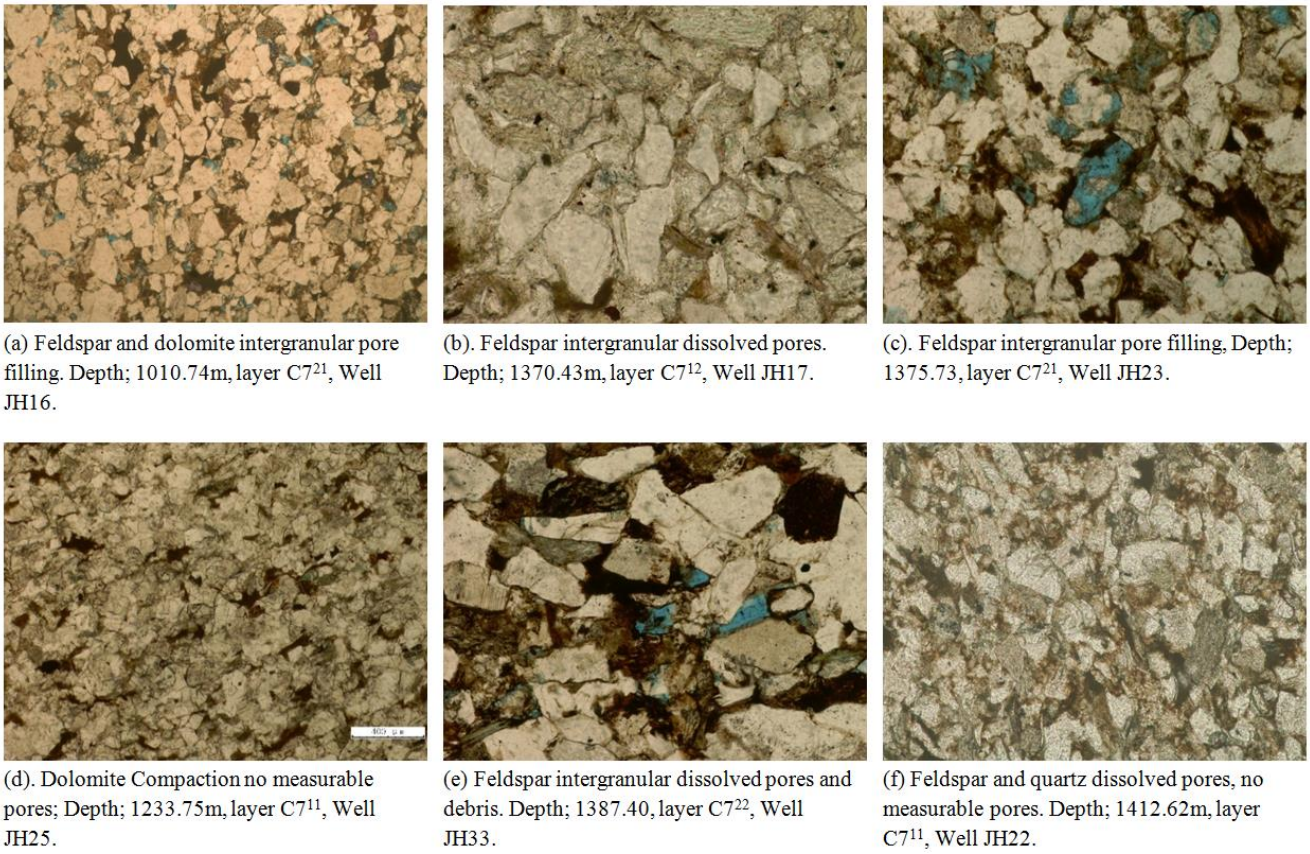

(a) Feldspar and dolomite intergranular pore filling. Depth; 1010.74m, layer $C7^{21}$, Well JH16.

(b). Feldspar intergranular dissolved pores. Depth; 1370.43m, layer $C7^{12}$, Well JH17.

(c). Feldspar intergranular pore filling, Depth; 1375.73, layer $C7^{21}$, Well JH23.

(d). Dolomite Compaction no measurable pores; Depth; 1233.75m, layer $C7^{11}$, Well JH25.

(e) Feldspar intergranular dissolved pores and debris. Depth; 1387.40, layer $C7^{22}$, Well JH33.

(f) Feldspar and quartz dissolved pores, no measurable pores. Depth; 1412.62m, layer $C7^{11}$, Well JH22.

Figure 11. *Thin section photographs of the diagenetic minerals in the C7 member of the Jinghe oilfield.*

4. Thickness Distribution and Depositional Facies of C7 Member

Facies construction by the sandstone thickness is an important constituent language of clastic rock, which confirm information to the sediment environment and deposition (Anderton 1985). The thickness distribution of the $C7^{11}$ layer sandstone was generated based on lithology achieved from the well-logging (Figure 12). The sediment distribution shows the thickness of the study oil interval differs within the different microfacies types. Six microfacies types were identified based on the thickness and depositional environment. These microfacies types include; sandy debris flow facies (SDF), sandy debris channel facies (SDC), Seismite-slump+trubidity (SST), seismite-slump sand sheet microfacies (SSS), turbidity sand sheet (TSS), and deepwater microfacies. On the whole the paleodeposition of the C7 Member controlled by gravity flow setting. Specifically, sandy debris flow and sandy debris channel microfacies are the major sources of sediment supply to the deep-water settings, they are primarily distributed in the shallow lake fan settings. The second dominant microfacies are the seismite-slump + turbidity current microfacies, these facies are controlled by sandy debris channel microfacies and distributed in a semi-deep lake environment. Seismite-slump sand sheet and turbidity current sand sheet are microfacies the minor, they distributed along with the deep-water fan. The sandstone thickness varies within the different layers, it shows a gradual decrease from a shallow lake to the deep-water environment. The thickest thickness flows with sandy debris flow facies followed by sandy debris channel facies, with the thickness ranges from 8 to 10>m thick. Seismite-slump+turbidity current microfacies show medium-thin sand body thickness, with a thickness of only 6m thick. Subsequently, microfacies of seismite-slump and turbidity current sand sheet shows the thickness of 2 to 4m thick. A thickness of less than 2 meter shows with the deep-water microfacies.

The sandy debris flow microfacies (SDF) and sandy debris channel facies (SDC) are the dominant sources that control thickness distribution and depositional facies during the period of the $C7^{11}$ layer. The major thickness and sediment accumulations show in the northwest with the thickness of 11.29m, at the well-JH43, and reach to the southeast region with a thickness of 10.32m at the well-JH9. Apparently, sandy debris channel facies (SDC) is the main sediment feeder, which provides the semi-deep water seismite-slump +

turbidity current microfacies (SST). The thickness of the sandy debris channel facies is more than 8m. In contrast, Seismite-slump+turbidity microfacies (SST) are largely settled near the semi-deep fan settings with a thickness of about 6.47m. Meanwhile, the deep-water seismite-slump and turbidity current sand sheets show minor facies with the thickness range from 2 to 4.38m. The depositional system of the $C7^{11}$ layer is controlled by gravity flows, where the sandy debris flow microfacies are the dominant source of the sediment supply and the seismite-slump and turbidity are the minor microfacies. The lake development in the $C7^{11}$ period is small. In the north and east sections, a small development of the lake entered, where the west section shows relativity higher development of the lake. The central region shows high accumulations of gravity flow sandstone, which make favourable conditions of oil-bearing.

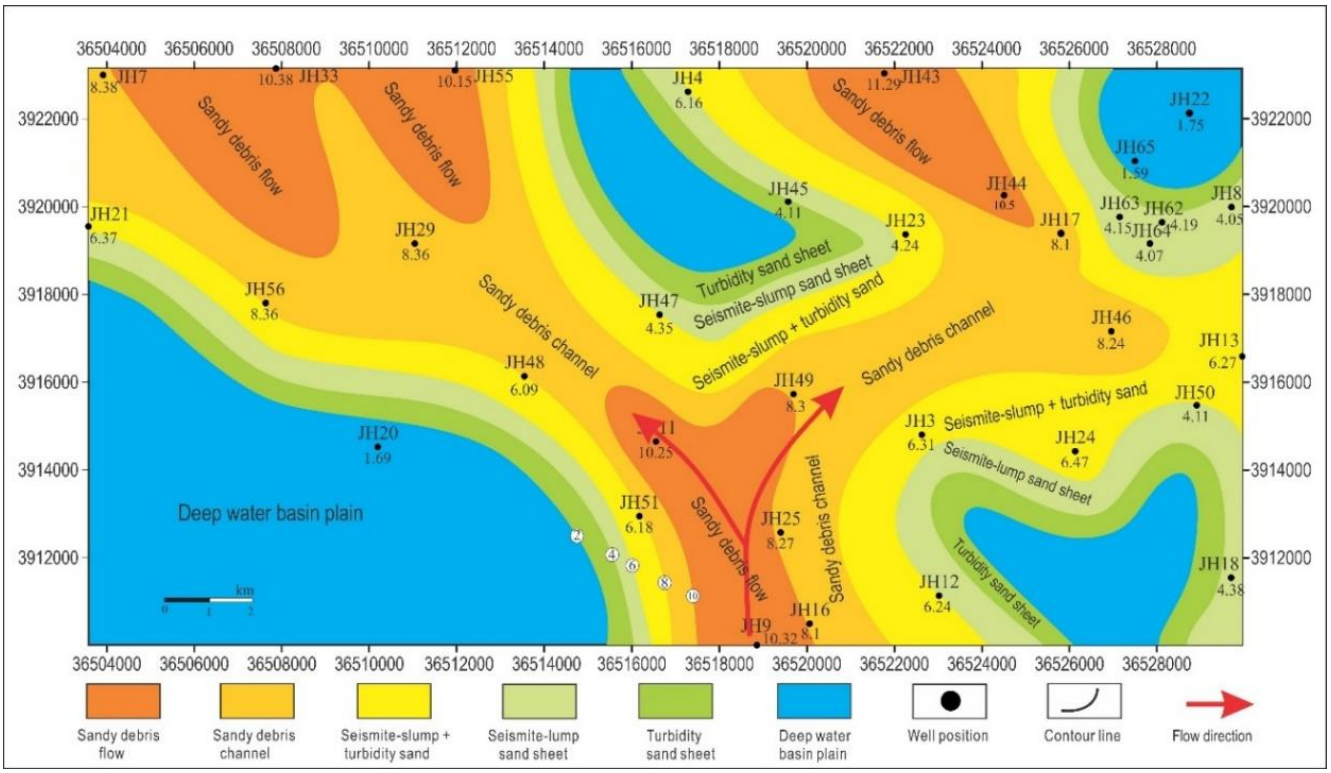

Figure 12. *Sandstone thickness distribution map of $C7^{11}$ layer of the C7 member.*

5. Conclusion

The late Triassic C7 member deep-water gravity flow reservoir of the Yanchang Formation in the Jinghe oilfield southern Ordos basin, microfacies facies differentiation controlled physical properties. Sandy debris flow microfacies shows the better porosity-permeability, followed by seismite-slump facies and turbidity microfacies. The overall properties distribution in the C7 member shows porosity distribution ranges from 0 to 18%, the average of 9%, and permeability ranges from 0.01 to 1mD with an average of 0.25mD, which believed to be a typical tight oil reservoir. Further, due the progressive pressure and burial, mineral composition of feldspar, illite, smectite, calcite, and dolomite have strongly influenced the sandstone pores. The main diagenetic processes influence the sandstone quality by dissolved pores of feldspar and compaction. Compaction and dolomite cementation mainly control the quality of the sandstones together resulting in the development of compacted sandstone with no pores. Kaolinite cement intergranular pores filling aggregations and transformation of smectite into illite influenced the sandstone pore structure, which leads in the reduction of porosity-permeability.

Abbreviations

SDF: Sandy debris flow.
SDC: Sandy debris channel.
SST: Seismite-slump turbidity.
SSS: Seismite-slump sand sheet.
TSS: Turbidity sand sheet.

Acknowledgments

The authors thank the three anonymous reviewers for the constructive suggestions for the reviewing and editing of the article.

Data Availability Statement

The data used in this paper was provided by the National Natural Science Foundation of China (No. 41402086), China National Science and Technology Major Project under Contract 2016ZX05048-001–01-CS and SINOPEC Huabei Company for the research, authorship, and/or publication of this article for study purpose.

Conflicts of Interest

The authors declare no conflicts of interest.

References

[1] Abid, I. A., R. Hesse and J. D. Harper (2004). Variations in mixed-layer illite/smectite diagenesis in the rift and post-rift sediments of the Jeanne d'Arc Basin, Grand Banks offshore Newfoundland, Canada. Canadian Journal of Earth Sciences 41(4): 401-429.

[2] Ali, S. A., W. J. Clark, W. R. Moore and J. R. Dribus (2010). Diagenesis and reservoir quality. Oilfield Review 22(2): 14-27.

[3] Anderton, R. (1985). Clastic facies models and facies analysis. Geological Society, London, Special Publications 18(1): 31-47.

[4] Bjørlykke, K. (2014). Relationships between depositional environments, burial history and rock properties. Some principal aspects of diagenetic process in sedimentary basins. Sedimentary Geology 301: 1-14.

[5] Covault, J. A. and B. W. Romans (2009). Growth patterns of deep-sea fans revisited: Turbidite-system morphology in confined basins, examples from the California Borderland. Marine Geology 265(1-2): 51-66.

[6] Dutton, S. P. and R. G. Loucks (2010). Reprint of: Diagenetic controls on evolution of porosity and permeability in lower Tertiary Wilcox sandstones from shallow to ultradeep (200–6700 m) burial, Gulf of Mexico Basin, USA. Marine and Petroleum Geology 27(8): 1775-1787.

[7] Fan, S., J.-G. Hou and N.-N. Su (2009). Model building for Chang-8 low permeability sandstone reservoir in the Yanchang formation of the Xifeng oil field. Mining Science and Technology (China) 19(2): 245-251.

[8] Fisher, Q. J., M. Casey, M. B. Clennell and R. J. Knipe (1999). Mechanical compaction of deeply buried sandstones of the North Sea. Marine and Petroleum Geology 16(7): 605-618.

[9] Galloway, W. E. (1979). Diagenetic control of reservoir quality in arc-derived sandstones implications for petroleum exploration.

[10] Gier, S., R. H. Worden, W. D. Johns and H. Kurzweil (2008). Diagenesis and reservoir quality of Miocene sandstones in the Vienna Basin, Austria. Marine and Petroleum Geology 25(8): 681-695.

[11] Haile, B., T. Klausen, U. Czarniecka, K. Xi, J. Jahren and H. Hellevang (2018). How are diagenesis and reservoir quality linked to depositional facies? A deltaic succession, Edgeøya, Svalbard. Marine and Petroleum Geology 92: 519-546.

[12] Helmold, K. P. (2016). SEDIMENTARY PETROLOGY AND RESERVOIR QUALITY OF ALBIAN–CENOMANIAN NANUSHUK FORMATION SANDSTONES, USGS WAINWRIGHT# 1 TEST WELL, WESTERN NORTH SLOPE, ALASKA. Report of Investigations: 3.

[13] Hua, Y., X. LIANG, N. Xiaobing, F. Shengbin and Y. Yuan (2017). Geological conditions for continental tight oil formation and the main controlling factors for the enrichment: A case of Chang 7 Member, Triassic Yanchang Formation, Ordos Basin, NW China. Petroleum Exploration and Development 44(1): 11-19.

[14] Hurst, A. and P. H. Nadeau (1995). Clay microporosity in reservoir sandstones: an application of quantitative electron microscopy in petrophysical evaluation. AAPG bulletin 79(4): 563-573.

[15] Ji, L.-m., F.-w. Meng, J. D. Schiffbauer, J.-l. Xu, K. Yan and J.-w. Shu (2008). Correlation between highly abundant oil-prone leiosphaerid acritarchs and hydrocarbon source rocks from the Triassic Yanchang Formation, eastern Gansu Province, Northwestern China. Gondwana Research 14(3): 554-560.

[16] Jian, Y., Y. Yajuan and D. Jinliang (2010). Sedimentation during the transgression period in late Triassic Yanchang formation, Ordos Basin. Petroleum Exploration and Development 37(2): 181-187.

[17] Ketzer, J., S. Morad, A. Amorosi and R. Worden (2003). Predictive diagenetic clay-mineral distribution in siliciclastic rocks within a sequence stratigraphic framework. Clay mineral cements in sandstones, International Association of Sedimentologists Special Publication. 34: 43-61.

[18] Kilda, L. and H. Friis (2002). The key factors controlling reservoir quality of the Middle Cambrian Deimena Group sandstone in West Lithuania. Bulletin of the Geological Society of Denmark 49(1): 25-39.

[19] Li, Q., Z. Jiang, K. Liu, C. Zhang and X. You (2014). Factors controlling reservoir properties and hydrocarbon accumulation of lacustrine deep-water turbidites in the Huimin Depression, Bohai Bay Basin, East China. Marine and Petroleum Geology 57: 327-344.

[20] Lien, T., R. E. Midtbø and O. J. Martinsen (2006). Depositional facies and reservoir quality of deep-marine sandstones in the Norwegian Sea. Norwegian Journal of Geology/Norsk Geologisk Forening 86(2).

[21] Liu, L., H. Chen, Y. Zhong, J. Wang, C. Xu, A. Chen and X. Du (2017). Sedimentological characteristics and depositional processes of sediment gravity flows in rift basins: The Palaeogene Dongying and Shahejie formations, Bohai Bay Basin, China. Journal of Asian Earth Sciences 147: 60-78.

[22] Liu, X.-X., X.-Q. Ding, S.-N. Zhang and H. He (2017). Origin and depositional model of deep-water lacustrine sandstone deposits in the 7th and 6th members of the Yanchang Formation (Late Triassic), Binchang area, Ordos Basin, China. Petroleum Science 14(1): 24-36.

[23] Luo, J., J. Li, B. Yang, Y. Dai, B. Li, Y. Han, H. Wang and J. Du (2007). Provenance for the Chang 6 and Chang 8 Member of the Yanchang Formation in the Xifeng area and in the periphery Ordos Basin: Evidence from petrologic geochemistry. Science in China Series D: Earth Sciences 50(2): 75-90.

[24] Mansurbeg, H., S. Morad, A. Salem, R. Marfil, M. El-Ghali, J. Nystuen, M. Caja, A. Amorosi, D. Garcia and A. La Iglesia (2008). Diagenesis and reservoir quality evolution of palaeocene deep-water, marine sandstones, the Shetland-Faroes Basin, British continental shelf. Marine and Petroleum Geology 25(6): 514-543.

[25] Mayall, M., E. Jones and M. Casey (2006). Turbidite channel reservoirs—Key elements in facies prediction and effective development. Marine and Petroleum Geology 23(8): 821-841.

[26] McKinley, J., R. Worden, A. Ruffell and S. Morad (2003). Smectite in sandstones: a review of the controls on occurrence and behaviour during diagenesis. Clay Mineral Cements in Sandstones, International Association of Sedimentologists Special Publication. 34: 109-128.

[27] Oluwadebi, A. G., K. G. Taylor and P. J. Dowey (2018). Diagenetic controls on the reservoir quality of the tight gas Collyhurst sandstone formation, lower Permian, east Irish Sea basin, United Kingdom. Sedimentary Geology 371: 55-74.

[28] Poursoltani, M. R. and M. R. Gibling (2011). Composition, porosity, and reservoir potential of the Middle Jurassic Kashafrud Formation, northeast Iran. Marine and Petroleum Geology 28(5): 1094-1110.

[29] Qiu, X., C. Liu, G. Mao, Y. Deng, F. Wang and J. Wang (2014). Late Triassic tuff intervals in the Ordos basin, Central China: Their depositional, petrographic, geochemical characteristics and regional implications. Journal of Asian Earth Sciences 80: 148-160.

[30] Renchao, Y., H. Zhiliang, Q. Guiqiang, J. Zhijun, S. Dongsheng and J. Xiaohui (2014). A Late Triassic gravity flow depositional system in the southern Ordos Basin. Petroleum Exploration and Development 41(6): 724-733.

[31] Richards, M., M. Bowman and H. Reading (1998). Submarine-fan systems I: characterization and stratigraphic prediction. Marine and Petroleum Geology 15(7): 689-717.

[32] Schmid, S., R. Worden and Q. Fisher (2004). Diagenesis and reservoir quality of the Sherwood Sandstone (Triassic), Corrib field, Slyne basin, west of Ireland. Marine and Petroleum Geology 21(3): 299-315.

[33] Shanmugam, G. and R. Moiola (1988). Submarine fans: characteristics, models, classification, and reservoir potential. Earth-Science Reviews 24(6): 383-428.

[34] Songtao, W., Z. Rukai, C. Jinggang, C. Jingwei, B. Bin, X. Zhang, J. Xu, Z. Desheng, Y. Jianchang and L. Xiaohong (2015). Characteristics of lacustrine shale porosity evolution, Triassic Chang 7 member, Ordos Basin, NW China. Petroleum Exploration and Development 42(2): 185-195.

[35] Taylor, T. R., M. R. Giles, L. A. Hathon, T. N. Diggs, N. R. Braunsdorf, G. V. Birbiglia, M. G. Kittridge, C. I. Macaulay and I. S. Espejo (2010). Sandstone diagenesis and reservoir quality prediction: Models, myths, and reality. AAPG bulletin 94(8): 1093-1132.

[36] Vinchon, C., D. Giot, F. Orsag-Sperber, F. Arbey, J. Thibieroz, P. Cros, D. Jeannette and J.-P. Sizun (1996). Changes in reservoir quality determined from the diagenetic evolution of Triassic and Lower Lias sedimentary successions (Balazuc borehole, Ardèche, France). Marine and petroleum geology 13(6): 685-694.

[37] von Eynatten, H., C. Barceló-Vidal and V. Pawlowsky-Glahn (2003). Composition and discrimination of sandstones: a statistical evaluation of different analytical methods. Journal of Sedimentary Research 73(1): 47-57.

[38] Wang, G., X. Chang, W. Yin, Y. Li and T. Song (2017). Impact of diagenesis on reservoir quality and heterogeneity of the Upper Triassic Chang 8 tight oil sandstones in the Zhenjing area, Ordos Basin, China. Marine and Petroleum Geology 83: 84-96.

[39] Xi, K., Y. Cao, J. Jahren, R. Zhu, K. Bjørlykke, B. G. Haile, L. Zheng and H. Hellevang (2015). Diagenesis and reservoir quality of the Lower Cretaceous Quantou Formation tight sandstones in the southern Songliao Basin, China. Sedimentary geology 330: 90-107.

[40] Xian, B., J. Wang, C. Gong, Y. Yin, C. Chao, J. Liu, G. Zhang and Q. Yan (2018). Classification and sedimentary characteristics of lacustrine hyperpycnal channels: Triassic outcrops in the south Ordos Basin, central China. Sedimentary Geology 368: 68-82.

[41] Yanru, G., L. Junbang, Y. Hua, L. Zhen, F. Jinhua, Y. Jingli, X. Wanglin and Y. ZHANG (2012). Hydrocarbon accumulation mechanism of low permeable tight lithologic oil fields in the Yanchang Formation, Ordos Basin, China. Petroleum Exploration and Development 39(4): 447-456.

[42] Zhang, J., S. Wu, X. Wang, Y. Lin, H. Fan, L. Jiang, Q. Wan, H. Yin and Y. Lu (2015). Reservoir quality variations within a sinuous deep-water channel system in the Niger Delta Basin, offshore West Africa. Marine and Petroleum Geology 63: 166-188.

[43] Zhenglong, Z., W. Guiwen, R. Ye, L. Jin, C. Yufeng and Z. Xianling (2016). A logging identification method of tight oil reservoir lithology and lithofacies: A case from Chang7 Member of Triassic Yanchang Formation in Heshui area, Ordos Basin, NW China. Petroleum Exploration and Development 43(1): 65-73.

[44] Zhongxing, L., Q. Xuefeng, L. Wantao, L. Qihong, S. Hualing and H. Youan (2015). Development modes of Triassic Yanchang formation Chang 7 member tight oil in Ordos Basin, NW China. Petroleum Exploration and Development 42(2): 241-246.

[45] ZHOU, J.-g., G.-s. YAO, H.-y. DENG, Y.-g. XIN, H. Heng, X.-p. ZHENG and Q.-s. GONG (2008). Exploration potential of Chang 9 member, Yanchang Formation, Ordos Basin. Petroleum Exploration and Development 35(3): 289-293.

[46] Zou, C., L. Wang, Y. Li, S. Tao and L. Hou (2012). Deep-lacustrine transformation of sandy debrites into turbidites, Upper Triassic, Central China. Sedimentary Geology 265: 143-155.